# Application of the thermal quadrupole method to the propagation of thermal waves in multilayered cylinders

Agustín Salazar[a)]
*Departamento de Física Aplicada I, Escuela Técnica Superior de Ingeniería, Universidad del País Vasco, Alameda Urquijo s/n, 48013 Bilbao, Spain*

Ricardo Celorrio
*Departamento de Matemática Aplicada, Universidad de Zaragoza, Campus Río Ebro, Edificio Torres Quevedo, 50018 Zaragoza, Spain*

(Received 10 July 2006; accepted 25 September 2006; published online 15 December 2006)

Up to now, research in photothermal techniques has been mainly restricted to samples with flat surfaces. In this work the surface temperature oscillation of multilayered cylindrical samples which are heated by a modulated light beam is calculated by using the quadrupole method. Different illumination geometries have been studied. Moreover, the lack of adherence between layers, as well as heat losses at the surface, has been considered in the model. Following this theoretical approach, photothermal techniques can be used for the quantitative thermophysical characterization of cylindrical samples with continuously varying in-depth thermal conductivity. © *2006 American Institute of Physics*. [DOI: 10.1063/1.2400403]

## I. INTRODUCTION

Photothermal techniques have become very powerful tools for the thermophysical characterization and nondestructive evaluation (NDE) of a wide variety of materials.[1] Photothermal wave techniques are based on the generation and detection of thermal waves in the sample under study. Thermal waves are generated in a material as a consequence of the absorption of an intensity modulated light beam. These highly damped thermal waves propagate through the material and are scattered by the buried heterogeneities. Different photothermal setups have been developed to detect these thermal waves and therefore to extract from them information on the thermal properties and internal structure of the material: infrared radiometry, mirage effect, photothermal reflectance, etc.

For decades, research in photothermal techniques has been restricted to samples with flat surfaces. Recently, some studies on cylindrical and spherical samples have been published.[2–4] In this work we calculate, using the quadrupole method, the surface temperature of a multilayered cylindrical sample which is heated by a modulated light beam. The quadrupole method is a unified exact method of representing linear systems. It has been applied in the framework of conductive transfer to calculate the surface temperature of flat multilayered samples.[5] Here we exploit this elegant method to express the surface temperature of multilayered cylindrical samples in a compact manner. Different illumination geometries have been studied, both with and without keeping the cylindrical symmetry. On the other hand, the lack of adherence between layers has been taken into account by introducing a thermal contact resistance. Moreover, heat losses at the surface have also been considered. Consequently, it is expected that this theoretical approach encourages the use of photothermal techniques for the quantitative thermophysical characterization of cylindrical samples with continuously varying in-depth thermal conductivity, as is the case of hardened steel wires, tubes, and nails.

## II. THEORY

In this section we first apply the quadrupole method to calculate the surface temperature of a multilayered cylinder that is illuminated by a light beam with cylindrical symmetry, modulated at a frequency $f$ ($\omega=2\pi f$). Accordingly, in this simple configuration the one-dimensional approach can be used. Then we generalize the method to include illuminations with no cylindrical symmetry, which are of more practical interest.

### A. Illumination with cylindrical symmetry

#### 1. A hollow cylinder

Let us consider an infinite, homogeneous, and opaque hollow cylinder with an outer radius $a$ and an inner radius $b$, which is uniformly illuminated by a radial light beam of intensity $I_0$ modulated at a frequency $f$. Its cross section is shown in Fig. 1(a). Due to the cylindrical symmetry of the illumination the temperature oscillation at any point of the cylinder can be written as[6,7]

$$T(r) = PJ_0(qr) + QH_0(qr), \tag{1}$$

where $q=\sqrt{i\omega/D}$ is the thermal wave vector, with $D$ the thermal diffusivity of the sample and $J_0$ and $H_0$ are the zeroth order of the Bessel and Hankel functions of the first kind, respectively. The first term in Eq. (1) represents the ingoing cylindrical thermal wave starting at the sample surface, while the second one is the corresponding reflected wave at the inner surface. $P$ and $Q$ are two constants to be determined according to the boundary conditions. On the other hand, if we define $j$ as minus the heat flux at any point of the cylinder, then it writes

a)Electronic mail: agustin.salazar@ehu.es

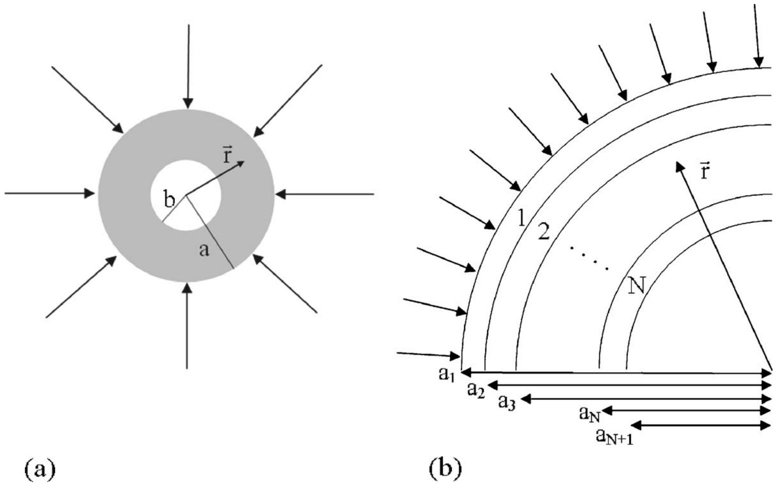


FIG. 1. Cross section of (a) a semi-infinite and opaque hollow cylinder and (b) a multilayered cylinder with an illumination with cylindrical symmetry.

$$j(r) = K\frac{dT}{dr} = Kq[PJ_0'(qr) + QH_0'(qr)], \tag{2}$$

where $K$ is the thermal conductivity of the sample and $J_0'$ and $H_0'$ are the derivatives of the Bessel and Hankel functions, respectively. The constants $P$ and $Q$ can be easily eliminated from Eqs. (1) and (2) by taking the values of temperature and heat flux at both surfaces ($r=a$ and $r=b$). In this way, a linear relation between temperature and flux at the outer and inner surfaces is obtained that can be expressed in the following matrix form:

$$\begin{pmatrix} T(a) \\ j(a) \end{pmatrix} = \begin{pmatrix} A & B \\ C & D \end{pmatrix} \begin{pmatrix} T(b) \\ j(b) \end{pmatrix}, \tag{3}$$

with

$$A = [H_0'(qb)J_0(qa) - J_0'(qb)H_0(qa)]/E,$$

$$B = [J_0(qb)H_0(qa) - H_0(qb)J_0(qa)]/EKq,$$

$$C = Kq[H_0'(qb)J_0'(qa) - J_0'(qb)H_0'(qa)]/E,$$

$$D = [J_0(qb)H_0'(qa) - H_0(qb)J_0'(qa)]/E$$

and

$$E = H_0'(qb)J_0(qb) - H_0(qb)J_0'(qb).$$

It is interesting to note that Eq. (3) is valid for any boundary condition at the surfaces. According to Eq. (3), if the heat flux at both surfaces is known, then the surface temperature can be obtained. For instance, for negligible heat losses $[j(a)=I_0/2$ and $j(b)=0]$ the surface temperature at both surfaces reduces to

$$T(a) = \frac{I_0}{2}\frac{A}{C}, \tag{4a}$$

$$T(b) = \frac{I_0}{2}\frac{1}{C}. \tag{4b}$$

On the other hand, when heat losses are present $[j(a)=I_0/2-h_aT(a)$ and $j(b)=h_bT(b)]$ the surface temperature writes

$$T(a) = \frac{I_0}{2}\frac{A+Bh_b}{C+Dh_b+Ah_a+Bh_ah_b}, \tag{5a}$$

$$T(b) = \frac{I_0}{2}\frac{1}{C+Dh_b+Ah_a+Bh_ah_b}, \tag{5b}$$

where $h_a$ and $h_b$ are the linearized heat transfer coefficients[5] at the outer and inner surfaces, respectively, which account for convective and radiative losses. Note that in the absence of heat losses ($h_a=h_b=0$) Eqs. (5) reduce to Eqs. (4). On the other hand, by making $b=0$ in Eq. (5a) and using the properties of the Bessel functions,[8,9] the surface temperature of a solid cylinder is obtained,

$$T(a) = \frac{I_0}{2}\frac{J_0(qa)}{KqJ_0'(qa)+h_aJ_0(qa)}. \tag{6}$$

It is worth noting that Eqs. (3)–(5) are the same as those obtained for a homogeneous and semi-infinite slab whose front surface is periodically illuminated by a uniform light beam,[5] but the coefficients $A$ to $D$ depend now on Bessel functions instead of on hyperbolic ones. That is the reason why we have used minus the heat flux instead of the heat flux itself.

### 2. A multilayered cylinder

Now we consider an infinite and opaque multilayered cylinder whose outer surface is uniformly illuminated by a radial light beam of intensity $I_0$ modulated at a frequency $f$. Its cross section is shown in Fig. 1(b). It is made of $N$ layers of different thicknesses and materials. The thermophysical properties of layer $i$ are labeled by subindex $i$ and its outer and inner radii by $a_i$ and $a_{i+1}$, respectively. According to the quadrupole method the temperature at the outer and inner surfaces of the cylinder, taking into account the influence of heat losses, are given by Eqs. (5),

$$T(a_1) = \frac{I_0}{2}\frac{A'+B'h_b}{C'+D'h_b+A'h_a+B'h_ah_b}, \tag{7a}$$

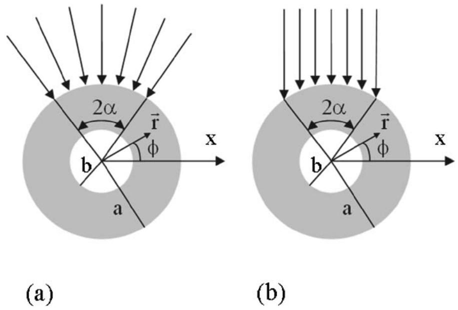


FIG. 2. Cross section of a semi-infinite and opaque hollow cylinder with two kinds of illumination with no cylindrical symmetry: (a) radial and (b) linear.

$$T(a_{N+1}) = \frac{I_0}{2}\frac{1}{C' + D'h_b + A'h_a + B'h_a h_b}, \tag{7b}$$

but now the transfer matrix to obtain the frequency dependent coefficients $A'$ to $D'$ is

$$\begin{pmatrix} A' & B' \\ C' & D' \end{pmatrix} = \prod_{i=1}^{N} \begin{pmatrix} A_i & B_i \\ C_i & D_i \end{pmatrix}, \tag{8}$$

with

$$A_i = [H_0'(q_i a_{i+1})J_0(q_i a_i) - J_0'(q_i a_{i+1})H_0(q_i a_i)]/E_i,$$

$$B_i = [J_0(q_i a_{i+1})H_0(q_i a_i) - H_0(q_i a_{i+1})J_0(q_i a_i)]/E_i K_i q_i,$$

$$C_i = K_i q_i [H_0'(q_i a_{i+1})J_0'(q_i a_i) - J_0'(q_i a_{i+1})H_0'(q_i a_i)]/E_i,$$

$$D_i = [J_0(q_i a_{i+1})H_0'(q_i a_i) - H_0(q_i a_{i+1})J_0'(q_i a_i)]/E_i$$

and

$$E_i = H_0'(q_i a_{i+1})J_0(q_i a_{i+1}) - H_0(q_i a_{i+1})J_0'(q_i a_{i+1}).$$

On the other hand, the lack of adherence between two adjacent layers can be accounted for by considering a very thin intermediate air layer. The thickness of this intermediate layer satisfies the condition $\ell_n = a_n - a_{n+1} \to 0$, and according to the asymptotic behavior of the Bessel functions,[8,9] the coefficients of the corresponding transfer matrix can be simplified as $A_n = D_n = 1$, $B_n = \ell_n / K_{\mathrm{air}} = R$, and $C_n = 0$. Here $R$ is the thermal contact resistance. This means that the effect of a thermal resistance between layers $i$ and $i+1$ $(R_{i,i+1})$ is accounted for by inserting in Eq. (8) the following matrix between the two adjacent matrices $i$ and $i+1$:

$$\begin{pmatrix} 1 & R_{i,i+1} \\ 0 & 1 \end{pmatrix}. \tag{9}$$

## B. Illumination with no cylindrical symmetry

The illumination we dealt with in the previous subsection is the easiest to be solved mathematically because of the cylindrical symmetry. However, this is difficult to fulfill in photothermal experiments. Accordingly we generalize the thermal quadrupole procedure to include two types of illumination with no cylindrical symmetry but with more practical application: a radial and a linear one (see Fig. 2). Both subtend the same angle $2\alpha$. In the first one [see Fig. 2(a)] the light intensity over the cylinder surface $g(\phi,\alpha)$ is $I_0$ for $\pi/2-\alpha \leqslant \phi \leqslant \pi/2+\alpha$ and zero for all other angles, and after being expanded in Fourier series writes

$$g(\phi,\alpha) = I_0 \sum_{m=-\infty}^{\infty} (-i)^m \frac{\sin(m\alpha)}{m\pi} e^{im\phi} = I_0 \sum_{m=-\infty}^{\infty} g_m(\alpha) e^{im\phi}. \tag{10}$$

In the second one [see Fig. 2(b)] the light intensity is $I_0 \sin\phi$ for $\pi/2-\alpha \leqslant \phi \leqslant \pi/2+\alpha$ and zero for all other angles, and expanded in Fourier series can be written as

$$\begin{aligned} g(\phi,\alpha) &= I_0 \sum_{m=-\infty}^{\infty} (-i)^m \\ &\quad\times \frac{m \sin(m\alpha)\cos\alpha - \sin\alpha\cos(m\alpha)}{\pi(m^2-1)} e^{im\phi} \\ &= I_0 \sum_{m=-\infty}^{\infty} g_m(\alpha) e^{im\phi}. \end{aligned} \tag{11}$$

### 1. A hollow cylinder

Let us consider the same hollow cylinder as in Sec. II A 1. Two light beams are considered whose cross sections are shown in Fig. 2. According to the loss of cylindrical symmetry, the temperature oscillation at any point of the cylinder is given by[6,7]

$$\begin{aligned} T(r,\phi) &= \sum_{m=-\infty}^{\infty} [P_m J_m(qr) + Q_m H_m(qr)] e^{im\phi} \\ &= \sum_{m=-\infty}^{\infty} t_m(r) e^{im\phi}, \end{aligned} \tag{12}$$

where $J_m$ and $H_m$ are the $m$th order of the Bessel and Hankel functions of the first kind, respectively. $P_m$ and $Q_m$ are $2m+1$ constants to be determined according to the boundary conditions. On the other hand, $j$ at any point of the cylinder writes

$$\begin{aligned} j(r,\phi) &= K\frac{\partial T}{\partial r} = Kq \sum_{m=-\infty}^{\infty} [P_m J_m'(qr) + Q_m H_m'(qr)] e^{im\phi} \\ &= \sum_{m=-\infty}^{\infty} f_m(r) e^{im\phi}, \end{aligned} \tag{13}$$

where $J_m'$ and $H_m'$ are the derivatives of the Bessel and Hankel functions, respectively. The $2m+1$ constants $P_m$ and $Q_m$ can be eliminated from Eqs. (10) and (11) by taking the values of $t_m$ and $f_m$ at both surfaces $(r=a$ and $r=b)$. In this way, a linear relation between $t_m$ and $f_m$ at the outer and inner surfaces is obtained that can be expressed in the following matrix form:

$$\begin{pmatrix} t_m(a) \\ f_m(a) \end{pmatrix} = \begin{pmatrix} A_m & B_m \\ C_m & D_m \end{pmatrix} \begin{pmatrix} t_m(b) \\ f_m(b) \end{pmatrix},$$

$$\forall m = -\infty, \ldots, 0, \ldots, \infty, \tag{14}$$

with

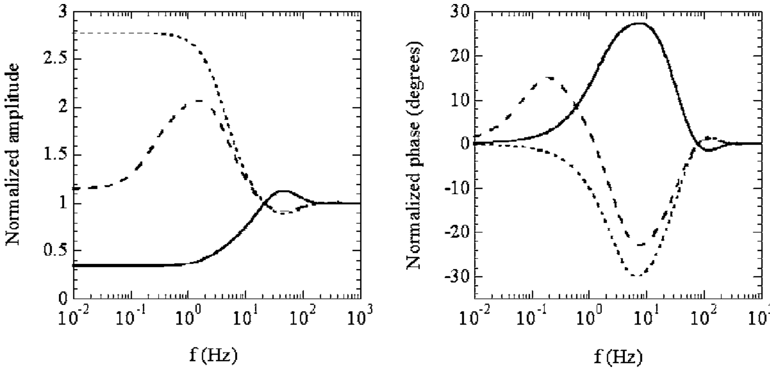


FIG. 3. Normalized amplitude and phase of the surface temperature of a two-layer cylinder whose radius is 1 mm and with an illumination with cylindrical symmetry. The outer layer is 0.2 mm thick made of AISI-304 stainless steel. Three different inner layers are considered: (a) a good thermal conductor ($K$=400 W m$^{-1}$ K$^{-1}$ and $D$=100 mm$^2$/s) (continuous line), (b) a thermal insulator ($K$=0.2 W m$^{-1}$ K$^{-1}$ and $D$=0.1 mm$^2$/s) (dashed line), and (c) air ($K$=0.026 W m$^{-1}$ K$^{-1}$ and $D$=22 mm$^2$/s) (dotted line).

$$A_m = [H_m'(qb)J_m(qa) - J_m'(qb)H_m(qa)]/E_m,$$

$$B_m = [J_m(qb)H_m(qa) - H_m(qb)J_m(qa)]/E_mKq,$$

$$C_m = Kq[H_m'(qb)J_m'(qa) - J_m'(qb)H_m'(qa)]/E_m,$$

$$D_m = [J_m(qb)H_m'(qa) - H_m(qb)J_m'(qa)]/E_m,$$

and

$$E_m = H_m'(qb)J_m(qb) - H_m(qb)J_m'(qb).$$

For negligible heat losses [$f_m(a)=I_0g_m(\alpha)/2$ and $f_m(b)=0, \forall m=-\infty,\ldots,0,\ldots,\infty$] the coefficients $t_m(a)$ and $t_m(b)$ are

$$t_m(a) = \frac{I_0}{2}g_m(\alpha)\frac{A_m}{C_m}, \tag{15a}$$

$$t_m(b) = \frac{I_0}{2}g_m(\alpha)\frac{1}{C_m}, \tag{15b}$$

and using Eq. (12) the surface temperature can be obtained,

$$T(a,\phi) = \frac{I_0}{2}\sum_{m=-\infty}^{\infty} g_m(\alpha)\frac{A_m}{C_m}e^{im\phi}, \tag{16a}$$

$$T(b,\phi) = \frac{I_0}{2}\sum_{m=-\infty}^{\infty} g_m(\alpha)\frac{1}{C_m}e^{im\phi}, \tag{16b}$$

where $g_m(\alpha)$ is taken from Eq. (10) or (11) according to the geometry of the illumination.

When heat losses are present [$f_m(a)=I_0g_m(\alpha)/2-h_at_m(a)$ and $f_m(b)=h_at_m(b), \forall m=-\infty,\ldots,0,\ldots,\infty$] the coefficients $t_m(a)$ and $t_m(b)$ are

$$t_m(a) = \frac{I_0}{2}g_m(\alpha)\frac{A_m+B_mh_b}{C_m+D_mh_b+A_mh_a+B_mh_ah_b}, \tag{17a}$$

$$t_m(b) = \frac{I_0}{2}g_m(\alpha)\frac{1}{C_m+D_mh_b+A_mh_a+B_mh_ah_b}, \tag{17b}$$

and from Eq. (12) the surface temperature is obtained,

$$T(a,\phi) = \frac{I_0}{2}\sum_{m=-\infty}^{\infty} g_m(\alpha)\frac{A_m+B_mh_b}{C_m+D_mh_b+A_mh_a+B_mh_ah_b}e^{im\phi}, \tag{18a}$$

$$T(b,\phi) = \frac{I_0}{2}\sum_{m=-\infty}^{\infty} g_m(\alpha)\frac{1}{C_m+D_mh_b+A_mh_a+B_mh_ah_b}e^{im\phi}. \tag{18b}$$

As a particular case, by making $b=0$ in Eq. (18a) and using the properties of the Bessel functions,[8,9] a simple expression for the surface temperature of a solid cylinder is obtained,

$$T(a,\phi) = \frac{I_0}{2}\sum_{m=-\infty}^{\infty} g_m(\alpha)\frac{J_m(qa)}{KqJ_m'(qa)+h_aJ_m(qa)}e^{im\phi}. \tag{19}$$

### *2. A multilayered cylinder*

Finally, we consider the same multilayered cylinder as in Sec. II A 2. Proceeding in a similar way as before, the temperature at any point of the outer and inner surfaces, taking into account the influence of heat losses, is given by Eqs. (18),

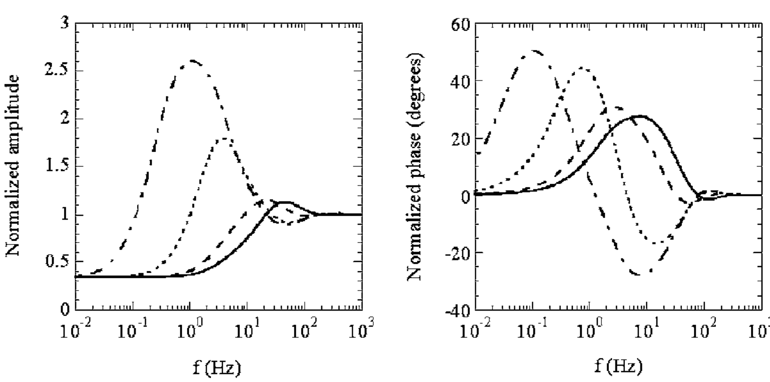


FIG. 4. Effect of the thermal resistance in the normalized amplitude and phase of the surface temperature of a two-layer cylinder whose radius is 1 mm and with an illumination with cylindrical symmetry. The outer layer is 0.2 mm thick made of AISI-304 stainless steel. The inner layer is made of a good thermal conductor ($K$=400 W m$^{-1}$ K$^{-1}$ and $D$=100 mm$^2$/s). (a) $R$=0 (continuous line), (b) $R$=10$^{-5}$ m$^2$ K W$^{-1}$ (dashed line), (c) $R$=10$^{-4}$ m$^2$ K W$^{-1}$ (dotted line), and (d) $R$=10$^{-3}$ m$^2$ K W$^{-1}$ (dashed-dotted line).

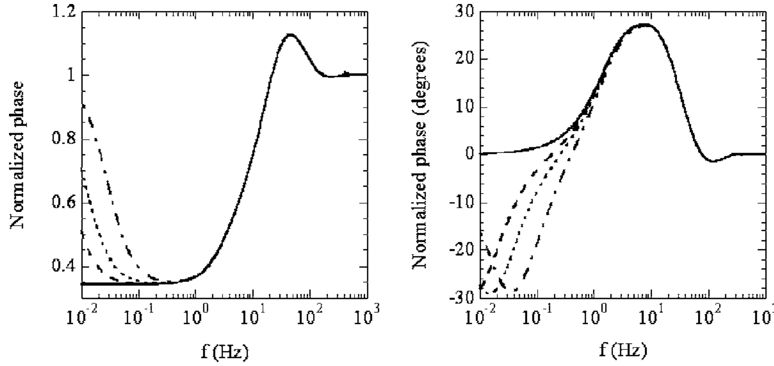


FIG. 5. Effect of heat losses in the normalized amplitude and phase of the surface temperature of the same two-layer cylinder as in Fig. 4. (a) $h=0$ (continuous line), (b) $h=100\ \mathrm{W\,m^{-2}\,K^{-1}}$ (dashed line), (c) $h=200\ \mathrm{W\,m^{-2}\,K^{-1}}$ (dotted line), and (d) $h=500\ \mathrm{W\,m^{-2}\,K^{-1}}$ (dashed-dotted line).

$$T(a_1,\phi)=\frac{I_0}{2}\sum_{m=-\infty}^{\infty} g_m(\alpha)\times\frac{A'_m+B'_m h_b}{C'_m+D'_m h_b+A'_m h_a+B'_m h_a h_b}e^{im\phi}, \quad (20a)$$

$$T(a_{N+1},\phi)=\frac{I_0}{2}\sum_{m=-\infty}^{\infty} g_m(\alpha)\times\frac{1}{C'_m+D'_m h_b+A'_m h_a+B'_m h_a h_b}e^{im\phi}, \quad (20b)$$

but now the $2m+1$ transfer matrices to obtain the frequency dependent coefficients $A'_m$ to $D'_m$ are

$$\begin{pmatrix} A'_m & B'_m \\ C'_m & D'_m \end{pmatrix}=\prod_{i=1}^{N}\begin{pmatrix} A_{mi} & B_{mi} \\ C_{mi} & D_{mi} \end{pmatrix}, \quad m=-\infty,\ldots,0,\ldots,+\infty, \quad (21)$$

with

$$A_{mi}=[H'_{mi}(q_ia_{i+1})J_{mi}(q_ia_i)-J'_{mi}(q_ia_{i+1})H_{mi}(q_ia_i)]E_{mi},$$

$$B_{mi}=[J_{mi}(q_ia_{i+1})H_{mi}(q_ia_i)-H_{mi}(q_ia_{i+1})J_{mi}(q_ia_i)]/E_{mi}K_iq_i,$$

$$C_{mi}=K_iq_i[H'_{mi}(q_ia_{i+1})J'_{mi}(q_ia_i)-J'_{mi}(q_ia_{i+1})H'_{mi}(q_ia_i)]/E_{mi},$$

$$D_{mi}=[J_{mi}(q_ia_{i+1})H'_{mi}(q_ia_i)-H_{mi}(q_ia_{i+1})J'_{mi}(q_ia_i)]/E_{mi}$$

and

$$E_{mi}=H'_{mi}(q_ia_{i+1})J_{mi}(q_ia_{i+1})-H_{mi}(q_ia_{i+1})J'_{mi}(q_ia_{i+1}).$$

As in the case of illumination with cylindrical symmetry, the influence of a bad adherence between layers $i$ and $i+1$ is accounted for by inserting in Eq. (21) the same matrix given by Eq. (9) between the two adjacent matrices $i$ and $i+1$.

## III. NUMERICAL CALCULATIONS AND DISCUSSION

As a test of consistency we have compared our solutions obtained from the quadrupole method to those previously published using Green's function method for a solid cylinder and for a two-layer cylinder which are illuminated as in Fig. 2(b).[2,3] Calculations of the surface temperature of a solid cylinder using our Eq. (19) and using Eq. (11) in Ref. 2 and of a bilayer cylinder using our Eq. (20a) and using Eq. (17) in Ref. 3 show the same results in the whole range of frequencies.

Now we calculate the surface temperature oscillation in a two-layer solid cylinder with a total radius of 1 mm, which is illuminated by a modulated light beam with cylindrical symmetry as that shown in Fig. 1(a). The outer layer is made of AISI-304 stainless steel ($K=10\ \mathrm{W\,m^{-1}\,K^{-1}}$ and $D=4\ \mathrm{mm^2/s}$) with a thickness of 0.2 mm. In all the simulations the surface temperature of the two-layer cylinder is normalized to a homogeneous stainless steel cylinder with the same radius as the bilayer one. In Fig. 3 the influence of the material of the inner layer on the amplitude and phase of the surface temperature is shown as a function of the modulation frequency. The continuous line represents the case of

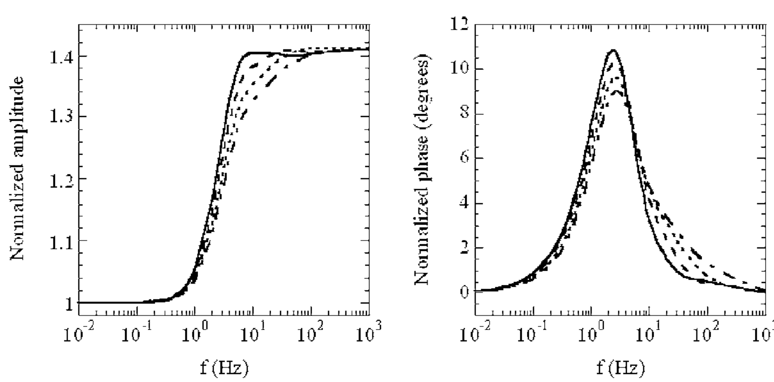


FIG. 6. Normalized amplitude and phase of the surface temperature of a multilayered cylinder whose radius is 1 mm and with an illumination with cylindrical symmetry. The inner core is made of AISI-304 stainless steel ($K=10\ \mathrm{W\,m^{-1}\,K^{-1}}$ and $D=4\ \mathrm{mm^2/s}$) and has a radius of 0.5 mm. In the outer part of the cylinder the transport thermal properties suffer from a continuously steplike decrease down to half of the core values at the surface ($K=5\ \mathrm{W\,m^{-1}\,K^{-1}}$ and $D=2\ \mathrm{mm^2/s}$). Four cases are considered: (a) two outer layers (continuous line), (b) three outer layers (dashed line), (c) five outer layers (dotted line), and (d) ten outer layers (dashed-dotted line).

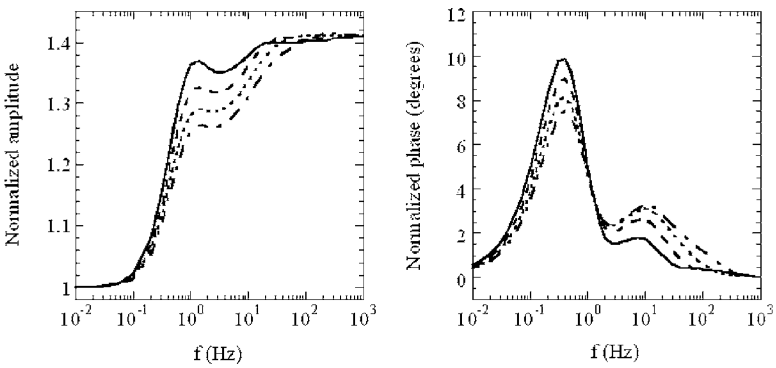


FIG. 7. The same as in Fig. 6, but now illuminated by a light beam with no cylindrical symmetry, as that shown in Fig. 2(b), with $\alpha=\pi/2$. The temperature is calculated at the north pole of the sample ($\phi=\pi/2$).

an inner layer made of a much better thermal conductor than the stainless steel ($K=400$ W m$^{-1}$ K$^{-1}$ and $D=100$ mm$^2$/s). As can be seen there is a decrease in the amplitude together with an increase in the phase. The dotted line corresponds to an inner air layer ($K=0.026$ W m$^{-1}$ K$^{-1}$ and $D=22$ mm$^2$/s), showing the opposite trend, i.e., an increase in amplitude and a decrease in phase. Finally, the dashed line stands for a thermal insulator ($K=0.2$ W m$^{-1}$ K$^{-1}$ and $D=0.1$ mm$^2$/s) that shows an intermediate behavior. These results are similar to those found in two-layer plates.[1] The influence in the surface temperature due to the presence of a thermal resistance between the two layers is shown in Fig. 4. The material is the same two-layer cylinder as in Fig. 3 with the inner layer made of a very good thermal conductor ($K=400$ W m$^{-1}$ K$^{-1}$ and $D=100$ mm$^2$/s). The continuous line represents a perfect thermal contact, the dashed line is for $R=10^{-5}$ m$^2$ K W$^{-1}$, the dotted line is for $R=10^{-4}$ m$^2$ K W$^{-1}$, and the dashed-dotted line for $R=10^{-3}$ m$^2$ K W$^{-1}$. As the thermal resistance increases both amplitude and phase differ from the perfect thermal contact, represented by the continuous line, and the temperature behaves as in the case of an inner insulator (see dashed line in Fig. 3). In Fig. 5 the influence of heat losses at the surface is shown. The bilayer cylinder is the same as in Fig. 4, with a perfect thermal contact between the core and coating. The continuous line represents the absence of heat losses and it is the same curve as the continuous line in Fig. 4. The influence of heat losses only appears at low frequencies and it is small even for high coefficients of heat losses ($h=100$–$500$ W m$^{-2}$ K$^{-1}$). This is due to the fact that stainless steel is quite a good thermal conductor and the influence of heat losses increases as the thermal conductivity of the material decreases.

Following with the same illumination we analyze the surface temperature of a multilayered cylinder. It has a radius of 1 mm, with an inner core of a radius of 0.5 mm made of AISI-304 stainless steel ($K=10$ W m$^{-1}$ K$^{-1}$ and $D=4$ mm$^2$/s). In the outer part of the cylinder the transport thermal properties suffer from a continuously steplike decrease down to half of the core values at the surface ($K=5$ W m$^{-1}$ K$^{-1}$ and $D=2$ mm$^2$/s). In Fig. 6 the normalized amplitude and phase of the surface temperature oscillation is shown as a function of the modulation frequency. Normalization is performed with respect to a homogeneous cylinder of the same size made of AISI-304 stainless steel. Four cases are considered: (a) two outer layers 0.25 mm thick each, (b) three outer layers 0.166 mm thick each, (c) five outer layers 0.10 mm thick each, and (d) ten outer layers 0.05 mm thick each. As the number of layers increases the shapes of both amplitude and phase are similar but shifted to higher frequencies. Moreover, the highest phase contrast is reduced. This is due to the fact that as the number of layers increases the thermal contrast reduces and therefore the amplitude of the reflected thermal wave becomes smaller. Note that as the number of layers goes to infinity this model simulates the case of a heterogeneous material with continuously varying thermal properties, as is the case of samples affected by surface modifying processes, e.g., steel hardening, annealing, etc. However, as in the case of flat layered systems, the convergence is very slow and many layers are necessary to guarantee the convergence.[10]

Now we study the same multilayered sample of Fig. 6 but illuminated with a light beam with no cylindrical symmetry [as that shown in Fig. 2(b)] with $\alpha=\pi/2$. In Fig. 7 we show the frequency scan of the normalized amplitude and phase of the surface temperature as measured at the north pole of the sample ($\phi=\pi/2$). Three differences with respect to Fig. 6 can be pointed out: (a) a double peak structure, both in amplitude and phase, (b) a shift to lower frequencies, and (c) a reduction of the highest phase contrast. In Fig. 8 we show the south pole temperature ($\phi=-\pi/2$) as a function of the square root frequency. As in the case of flat layers a linear behavior has been found, but a simple relation between its slope and the effective thermal properties of the multilayered cylinder has not been found. As can be seen, as

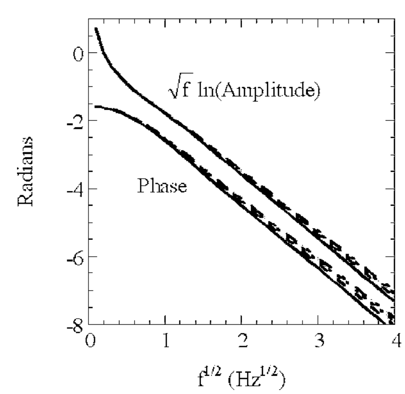


FIG. 8. The same sample and illumination as in Fig. 7, but now the temperature is calculated at the south pole of the sample ($\phi=-\pi/2$).

the number of layers increases the slope does in agreement with the corresponding increase of the effective thermal properties of the sample.

It is worth noting that using the inverse Laplace transform,[5] the modulated solutions presented in Sec. II can be used to calculate the temperature evolution of multilayered cylinders after being heated by a short duration light pulse. This means that this theoretical approach can be used in both lock-in and pulsed infrared thermographies.

In this work an extension of the thermal quadrupole method to calculate the surface temperature of multilayered cylindrical samples has been presented. It is expected that this theoretical approach encourages the use of photothermal techniques for the quantitative thermophysical characterization of coated cylinders and hardened steel cylindrical samples such as thin wires, tubes, and nails.

## ACKNOWLEDGMENT

This work has been supported by the Ministerio de Educación y Ciencia through research Grant No MAT2005-02999.

[1] D. P. Almond and P. M. Patel, *Photothermal Science and Techniques* (Chapman and Hall, London, 1996).
[2] C. Wang, A. Mandelis, and Y. Liu, J. Appl. Phys. **96**, 3756 (2004).
[3] C. Wang, A. Mandelis, and Y. Liu, J. Appl. Phys. **97**, 014911 (2005).
[4] A. Salazar, F. Garrido, and R. Celorrio, J. Appl. Phys. **99**, 066116 (2006).
[5] D. Maillet, S. André, J. C. Batsale, A. Degiovanni, and C. Moyne, *Thermal Quadrupoles* (Wiley, New York, 2000).
[6] J. Sinai and R. C. Waag, J. Acoust. Soc. Am. **83**, 1729 (1988).
[7] Y. S. Joo, J. G. Ih, and M. S. Choi, J. Acoust. Soc. Am. **103**, 900 (1998).
[8] *Handbook of Mathematical Functions*, edited by M. A. Abramowitz and I. A. Stegun (National Bureau of Standards, Washington DC, 1964).
[9] G. Arfken and H. J. Weber, *Mathematical Methods for Physicists*, 6th ed. (Academic, New York, 2005).
[10] R. Kolarov and T. Velinov, J. Appl. Phys. **83**, 1878 (1998).